

# Stability and Safety Analysis of the Air Lifted Catamaran

Dracos Vassalos, *Universities of Glasgow and Strathclyde*

Nan Xie, *Universities of Glasgow and Strathclyde*

Andrzej Jasionowski, *Universities of Glasgow and Strathclyde*

## ABSTRACT

The Air Lifted Catamaran (ALC) is an innovative fast marine transportation concept, comprising the application and variation of a new, skirtless air cushion and air-lubrication, thus rendering it a hybrid between catamaran and SES (Surface Effect Ship). Its features and capabilities are beyond current conventional high-speed mono-hull and catamaran. The present paper presents pertinent studies on stability concerning this craft, including dynamic stability, stability in turning and directional stability. The stability analysis takes into account air compressibility in the cushion, and is carried out in time domain. Some simulated results are presented and discussed, and requirements for design and operation of the craft based on IMO HSC Code 2000 are briefly outlined.

**Keywords:** *stability; air lifted vehicle; numerical simulation;*

## 1. INTRODUCTION

Conventional fast catamarans and mono-hulls have in the last few years gradually increased their operational speed, but at the cost of larger installed engines, burning more fuel and costing considerably more, to install, maintain and operate. The design speed of the Air Lifted Catamaran (ALC) is based upon speed capability of 70 knots for the 40m-long/350 passenger – fast ferry application, and operational speed of 50 knots for a 150m express cargo ship. Model tests have shown that its high-speed power reduction is around 25% when compared with the best of catamaran and mono-hull vessels, Allenstrom et al (2001), Allenstrom et al (2003). The present paper intends to address stability and safety issues of the ALC.

Recent international regulatory developments pertaining to high-speed craft, particularly the 2000 HSC code, acknowledge the necessity of

improvements of maritime safety standards for HSC in order to maintain the highest practical level of safety (IMO, 2000). However, the continuous update of stability rules and regulations for advanced high speed vessels compared to conventional vessels is greatly influenced by the fact that there are many different types of high speed vehicles, and many different alternative design solutions within each category, so a meaningful way to set safety and operational standards is to use performance based criteria and safety levels to which any type of craft must comply with.

The dynamic instability of high-speed craft has been known to lead to such violent motions that would cause serious accidents. With increasing vessel speed, this is becoming more and more a problem to the designers and operators (Vassalos, 1995). Papaniklaou et al have carried out an investigation of adaptation of stability rules and tools to SES (Papanikolaou, Georgantzi and Karayannis, 2002). In the present paper, a mathematical model is presented for the dynamic stability

---

analysis based on the features of the vessel. The mathematic model takes into account the air compressibility in the cushion (with the adiabatic gas law), and hydrodynamic forces coupled with the vessel motions. The free surface elevation in time domain induced by air pressure inside the cushion and at the periphery is represented in the form of convolution integrals, whose impulse response functions are calculated by the transfer functions of the moving pressure distributions in the frequency domain. Hydrodynamic forces acting on the rigid side-hull are calculated by a strip theory approximation in which the memory effect is also taken into account. The resulting non-linear equations of motions are solved using a Runge-Kutta scheme in time domain.

A number of case studies have been carried out for various design configurations of the ALC with the present code. A porpoising type of unstable phenomena has been identified for this type of vessel, which coincides with model experiments. The stable/unstable boundaries can be found with the present tool for different hull designs (such as cushion configurations, separation of the demi-hull, etc.), characteristics of inflow fan system and loading conditions (position of centre of gravity of the vessel) at various vessel speeds. The method developed in the present paper can be expected to be one of the tools for design of this type of vessel.

## 2. STATIC STABILITY OF THE AIR LIFTED CATAMARAN

### 2.1 The Vessel

The design feature of the ALC is similar, in some sense, to that of an SES catamaran. There are two demi-hulls, each of which contains air cushion(s). A forward planing surface ahead of the step creates some limited dynamic lift. The step and the forward planing surface also create the forward sealing of the air cushion chamber, the step being located in a plane close to

horizontal (no part of the step is to ventilate before the other). The bow section is slender in order to reduce displacement forces in a seaway, and the bow incorporate a voluminous part above a built-in chine/spray rail to reduce water deflection and reserve buoyancy in pitching motion. The side keels of varying height extend from just ahead of the step to the transom. The height of the keels is adjusted to the observed/expected shape of the air cushion. The only purpose of the side keels is to fence in the air cushion. There are spray rails on the outside of the side keels, at a height partly to deflect the water without wetting the rails on the upper sides. The cushion ceiling is at a height to avoid the sea hitting it when the vessel is moving in a seaway. There is a slope of the ceiling aft end in order to deflect passing waves in a seaway. A flap or enclosure arrangement in line with the sloped portion of the ceiling is arranged to fence the air cushion chamber in the rear part and to create dynamic lift and motion damping. Figure 1 shows the ALC concept E40.

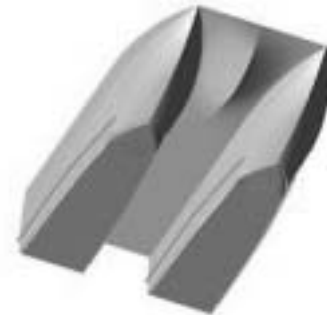


Figure 1 The E40 ALC concept (Allenstrom et al, 2001)

### 2.2 Static Stability

The vessel has basically two operational conditions: on-cushion (cushion-borne) mode and off-cushion (hull-borne) mode. Although the major operation of the ALC involves the cushion-borne mode, the hull-borne operation should also be considered. This is necessary as a result of safety and survivability requirements since it is possible that there may be times where a failure occurs in either the lift system or the seals, which would result in the vessel

operating in the hull-borne mode. In addition, during very severe sea conditions, it may be necessary for the ALC craft to operate only in the hull-borne mode for survival purposes. Also, there may be certain situations wherein purely hull-borne operation is considered for the vessel, dependent upon the degree of buoyancy initially designed for the sidewalls, for fuel conservation prior to a high-speed on-cushion mode in response to particular commands. In view of all these possibilities, it is therefore necessary to develop appropriate means of analysis and prediction of hull-borne motions in waves. The methods of analysis of hull-borne stability in this case follow the techniques applied to a displacement ship, using the software PROTEUS for this purpose; this will not be discussed in the present paper.

In the steady state condition, the balance of the vessel vertical force and moment about the transverse axis require:

$$\begin{cases} mg - 2A_c p_0 + \rho g \nabla + L_A + L_H = 0 \\ 2x_c A_c p_0 + x_B \rho g \nabla + x_{cA} L_A + x_{cH} L_H = 0 \end{cases} \quad (1)$$

where  $m$  is the mass of the vessel;  $L_A$  and  $L_H$  are hydrodynamic lift acting on the hull due to appendage and the craft hull itself;  $\nabla$  is buoyancy;  $A_c$  is cushion area of each demi-hull;  $p_0$  is the cushion excess pressure and  $\rho$  is water density.  $x_c$ ,  $x_B$ ,  $x_{cA}$  and  $x_{cH}$  are the longitudinal position of the centre of cushion pressure, buoyancy, appendage lift and hull lift, respectively.

Model test measurements have shown that the cushion excess pressure decreases with increasing vessel speed, which means that the cushion excess pressure will be lower at higher speed, the dynamic lift force playing a more important role. The two-phase fluid flow around the vessel is very complicated, accurate prediction of all those terms are difficult at present. Ideally, captive model tests at forward speed should be carried out to measure dynamic forces and moment acting on the hull, however, this is beyond the scope of the present study. T this end, some empirical

formulae are used. The fore body part and the stern flap are assumed to be lifting surfaces with different aspect ratios. The slopes of the lift force coefficients are taken from an aerofoil with finite aspect ratio.

In order to gain some basic understanding of the stability of the ALC, the metacentric height of the ALC at zero speed is evaluated. The procedure follows that of SES. (Blyth 1993, Faltinsen, 2002). The contributions of restoring moment from hydrostatic buoyancy of side hull and excess cushion chamber pressure are taken into account. For an ALC with side hulls of approximately constant section and wall-sided body surface at the free surface, the initial metacentric height will be:

$$\overline{GM} = \frac{1}{mg} [-2A_c p_0 (0.5h_0 + z_g) + 2\rho g A_c b_0^2 + \rho g S_{yy} - \rho g \nabla \overline{BG}] \quad (2)$$

where  $h_0$  is water head of the cushion excess pressure;  $b_0$  is the beam of cushion of demi-hull;  $S_{yy}$  is the transverse moment of inertia of water plane area of the ALC at on-cushion condition. The last two terms in the right hand side of (2) represent the metacentric height of normal catamaran. It can be seen that the excess pressure  $p_0$  in the cushion chamber gives a negative contribution to the metacentric height of the ALC. The second term in (2) is due to the catamaran configuration of the present ALC; for normal SES, this term vanishes. (Faltinsen, 2002).

Figure 2 shows an example of the static right lever of the ALC at zero speed. The displacement of the vessel is 170 tonnes and  $KG$  of 4m.

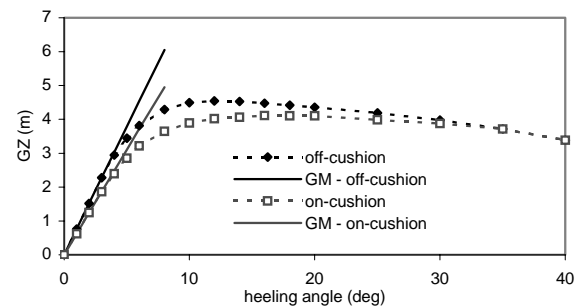


Figure 2 Static stability of an ALC at zero speed

### 3. DYNAMIC STABILITY ANALYSIS OF THE ALC

When the ALC is travelling at high speed, the analysis of the stability of the craft requires a dynamic model, which is presented in this section.

#### 3.1 The Mathematical Model

The dynamic behaviour of the vessel can be described as

$$[\mathbf{M}][\ddot{\mathbf{x}}] = [\mathbf{F}_H] + [\mathbf{F}_R] + [\mathbf{F}_P] + [\mathbf{F}_A] + [\mathbf{F}_W] \quad (3)$$

where  $\mathbf{M}$  is the matrix of inertia of the craft;  $\mathbf{F}_H, \mathbf{F}_R, \mathbf{F}_P, \mathbf{F}_A$  and  $\mathbf{F}_W$  are hydrodynamic force, hydrostatic force, cushion pressure force, appendage force and wave force, respectively.

The hydrodynamic forces/moments and wave forces acting on the vessel are calculated by PROTEUS3 with a radiation/diffraction method (Jasionowski, 2001). Appendage forces are calculated by an empirical formula, in which a quasi-steady-state assumption has been utilised. In order to get the equation of the cushion pressure for port and starboard chambers, the adiabatic gas law and the continuity equation in each chamber will be used:

$$\begin{cases} \frac{p_i + p_a + p_0}{\rho_i^\gamma} = \frac{p_a + p_0}{\rho_0^\gamma} \\ \frac{d}{dt}(\rho_i V_i) = \rho_a (Q_{in,i} - Q_{out,i}) \end{cases} \quad (4)$$

where the subscript "1" and "2" stand for port and starboard cushion chamber, respectively;  $Q_{in,i}$  is the inflow rate of the fan system,  $Q_{out,i}$  is the outflow rate of the cushion chamber.  $V_i$  is the instantaneous cushion volume, which is a function of craft motion, and free surface elevation in side cushion. The inflow flux of each fan system is normally a function of the cushion pressure. The out flow rate is given by

$$Q_{out,i}(t) = c_n A_{L,i}(t) \sqrt{\frac{2(p_i(t) + p_0)}{\rho_a}} \quad i=1,2 \quad (5)$$

where the instantaneous escape area,  $A_{L,i}(t)$ , at the periphery is

$$A_{L,i}(t) = \oint_{L,i} [z_{r,i}(x, y, t) + z_{r,i}(x, y, t)] dl \quad i=1,2 \quad (6)$$

where  $z_r$  is the local relative vertical motion between hull and free surface given by

$$z_r = z_0 + z - x\theta + y\phi - \zeta_w - \zeta_p \quad (7)$$

The free surface elevation due to cushion pressure is expressed as

$$\begin{cases} \zeta_p(x, y, t) = \int_0^t h_\zeta(x, y, \tau) p(t - \tau) d\tau \\ h_\zeta(x, y, \tau) = \frac{2}{\pi} \int_0^\infty H_{\zeta,r}(x, y, \sigma) \cos(\sigma\tau) d\sigma \end{cases} \quad (8)$$

where  $h_\zeta(x, y, \tau)$  is the impulse response function of the free surface elevation due to a unit cushion pressure. The free surface elevation transfer function,  $H_\zeta(x, y, \sigma)$ , is calculated by a pressure patch distribution method, in which the cushion area is represented by a number of rectangular pressure patches, see Figure 3. Full details of the formulation and numerical schemes can be found in Xie et al (Xie, Vassalos and Jasionowski, 2005a, 2005b),

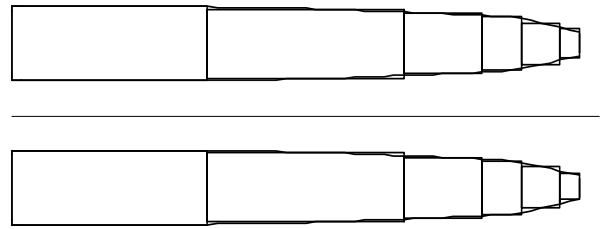


Figure 3 Representation of the cushion of the ALC

#### 3.2 Numerical Simulations

Given all the terms in the equation of motions, (4), simulations can be carried out in time domain. A Runge-Kutta scheme is

employed for the integration of the differential equations.

Much of the simulation work is on the numerical calculation of the impulse/transfer response functions of the free surface elevation. Previous research work published is either for lower frequency range (Doctors, 1974) or for relatively lower speed (Kim et al, 1981). The present simulation requires the whole frequency range as well as relatively high Froude number. Figure 4 shows a comparison of the free surface elevation for a rectangular pressure patch. Figure 5 shows a sample of escape volume of the ALC. Figures 6 and 7 show samples of free surface elevation transfer function, and Figure 8 shows a sample of impulse response functions of free surface at the stern of the ALC.

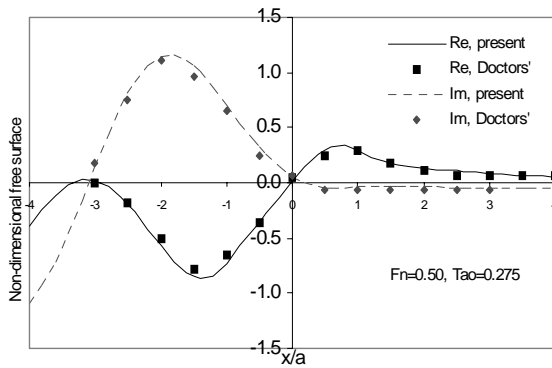


Figure 4 Wave-cut at  $y=b$  for a rectangular pressure patch ( $b/a=1, \tau=0.275, a$  = half length of pressure patch,  $b$  = half beam of the pressure patch)

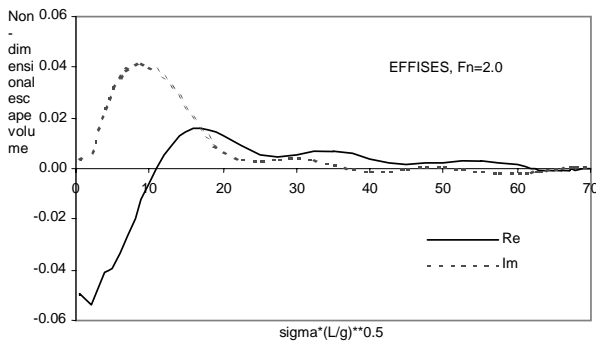


Figure 5 Samples of non-dimensional cushion escape volume

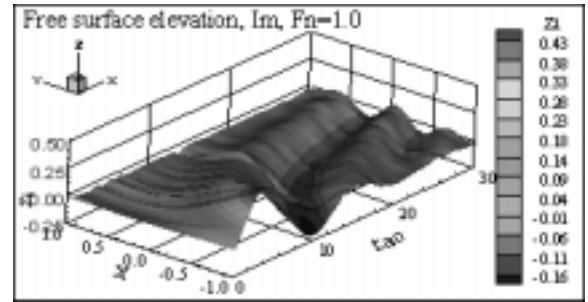


Figure 6 Transfer function of free surface elevation at  $Fr=1.0$  (imaginary part)

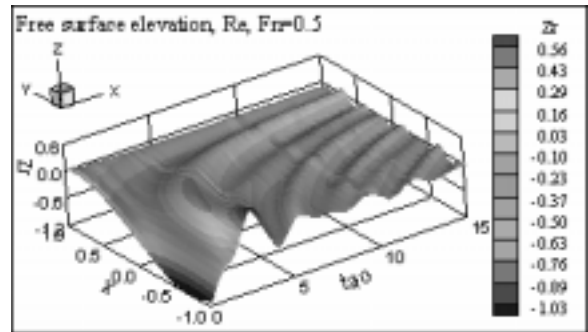


Figure 7 Transfer function of free surface elevation at  $Fr=0.5$  (real part)

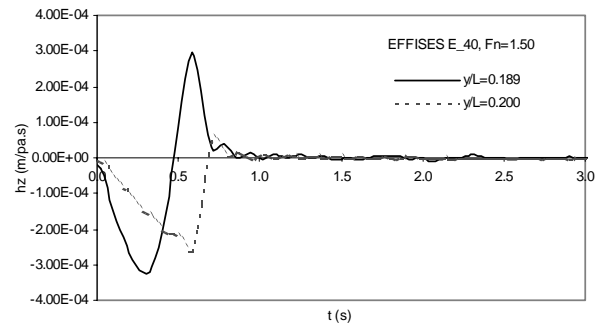


Figure 8 Impulse response function of free surface elevation of the ALC

Non-dimensional free surface elevation,  $\zeta$ , is defined as:

$$\zeta = \frac{\rho g \zeta}{\Pi} \quad (9)$$

Non-dimensional escape area and escape volume are defined as:

$$\tilde{A} = \frac{1}{L} \int_{y_1}^{y_2} \tilde{\zeta}(x_a, y; \sigma) dy \quad (10)$$

$$\tilde{V} = \frac{1}{L^2} \iint_{S_c} \tilde{\zeta}(x, y; \sigma) dx dy \quad (11)$$

respectively, where  $L$  is cushion length, and  $S_c$  is cushion area.

The dynamic stability in still water is simulated with the vessel undergoing motions subject to an initial position. This will lead to its equilibrant position in case of a stable condition, but the vessel motions will not decay in case of unstable conditions. Figure 9 shows some of the simulated results for the ALC craft E40, in which combinations of the craft design parameters are shown for the stable/unstable conditions. In the unstable cases, the simulated cushion pressure is divergent. It is found from the simulated results that, in the case of a craft with instability, the pressure in the cushions accumulates, cushion volume and craft motions increase, the escape of the accumulated air requires a large escape area, the pitch angle increases suddenly, and the cushion collapses like a cavity breaking down. This has been observed during model testing where in some unstable conditions, in which the cushion pressure collapses, with the C.G., inflow rate, fan slope characterises, stern flap, cushion height, etc., all affecting the stability of the craft. Typically, the craft is stable for the longitudinal position of C.G. within a limited range. A small inflow rate will increase chance of instability. Also the stern flap angle should be set properly to ensure the craft has a correct trim altitude and restoring moment at speed.

The longitudinal stability in waves can be analysed in the similar way. Figures 12 and 13 show samples of the simulated craft motions in waves.

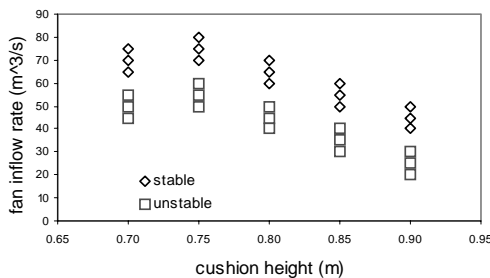


Figure 9 Sample of stable/unstable boundary of the ALC

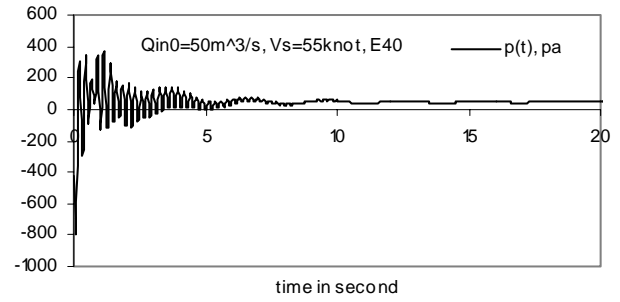


Figure 10 Sample of stable solution, cushion pressure

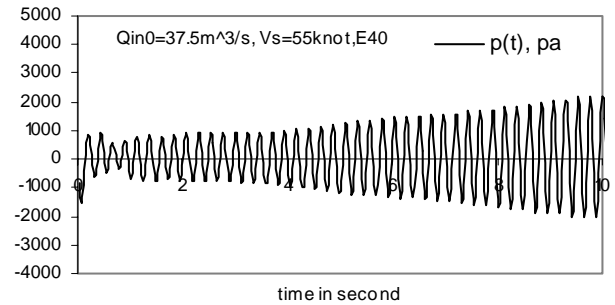


Figure 11 Sample of unstable solution, cushion pressure.

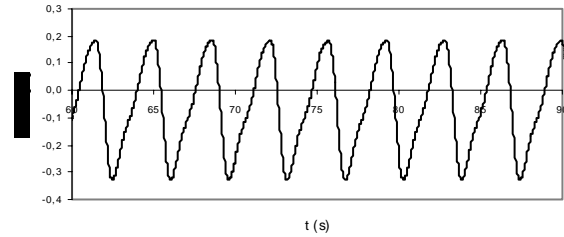


Figure 12 Simulated craft heave motion in waves

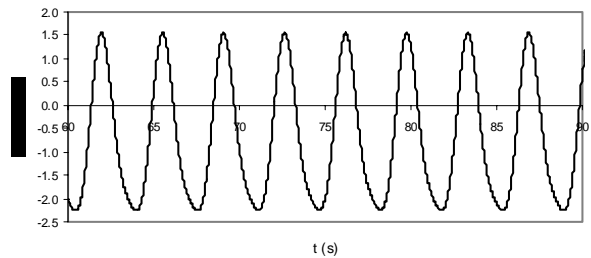


Figure 13 Simulated craft pitch motion in waves

#### 4. STABILITY OF THE ALC IN MANEUVERING

The stability of the ALC in high speed turning is an important aspect of stability performance. In the Annex 7 of HSC Code

2000 (IMO, 2000), the stability criteria in the intact condition requires that a multi-hull craft should have sufficient stability in high speed turning. Heeling due to high speed turning is calculated as follows:

$$TL = \frac{1}{g} \frac{U_0^2}{R} \left( KG - \frac{d}{2} \right) \quad (12)$$

where  $TL$  =turning level (m),  $U_0$  =speed of craft in turning (m/s),  $R$  =turning radius (m);  $KG$  =height of vertical centre of gravity above keel (m) and  $d$  =mean draught (m). In the present study, a mathematical model is presented for predicting the turning radius of the ALC.

#### 4.1 The Mathematical Model

Extending the description of craft motions to horizontal plane with four degrees of freedom, attention is paid to two translatory motion components along  $x$  (surge) and  $y$  (sway) axes, and to two angular motions about  $x$  –(roll) and  $z$  –(yaw) axes. The equations of motion in the body-fixed coordinate system are expressed as (Wade and Wang, 1977; Kaplan, 1995):

$$\begin{cases} m(\dot{u} - ru) = X \\ m(\dot{v} + rv) = Y \\ I_x \dot{p} = K \\ I_z \dot{r} = N \end{cases} \quad (13)$$

where  $u$  and  $v$  are linear velocity components of the craft C.G. along the body-fixed system;  $p$  and  $r$  are the angular velocities about  $x$  – and  $z$  –axes, respectively;  $X, Y, K, N$  are external forces/moments applied to the craft. Each component of the force/moment is assumed to be expressible by a summation of five independent contributions: inviscid, cross flow drag, cushion pressure force, wind force and the resulting effect propulsion and control, (Wade and Wang, 1977; Kaplan, 1995), as shown next.

$$\begin{cases} X = X_{invis} + X_{drag} + X_p + X_w + X_\delta \\ Y = Y_{invis} + Y_{drag} + Y_p + Y_w + Y_\delta \\ K = K_{invis} + K_{drag} + K_p + K_w + K_{buoy} + K_\delta \\ N = N_{invis} + N_{drag} + N_p + N_w + N_\delta \end{cases} \quad (14)$$

The inviscid hydrodynamic force and moment are calculated as follows. The total apparent velocity at the cross flow plane of rigid side hull is given by

$$V_r = v + \xi r - f(\xi) p \quad (15)$$

where  $f(\xi) = z_g - d(\xi)/2$  is the vertical distance of the centre of fluid pressure from the body C.G.; the 2-D added mass is  $\mu(\xi)$ , and the kinetic energy of a unit slice of the fluid

$$T(\xi, t) = \frac{1}{2} \mu(\xi) V_r^2(\xi) \quad (16)$$

The inviscid force/moment is then the change in the kinetic energy of the whole hull (integration along craft length). The cross-flow drag is:

$$Drag = -\frac{1}{2} \rho c_d s |V_r| V_r \quad (17)$$

where  $c_d$  = drag coefficient;  $s$  =project area. A water jet model is used (Wade and Wang, 1977). Wind force is calculated by formulae given by Aage (Aage, 1971).

Substituting all the external forces and moments into equations of motion, the linear and angular velocities can be obtained by solving the equation with a Runge-Kutta scheme, and the velocity components in the body fixed system are transformed to the earth fixed frame as shown next,

$$\begin{cases} \dot{x}_* = u \cos \psi - v \cos \varphi \sin \psi \\ \dot{y}_* = u \sin \psi + v \cos \varphi \cos \psi \\ \dot{\varphi} = p \\ \dot{\psi} = r / \cos \varphi \end{cases} \quad (18)$$

The solution of (15) give the trajectory of

the craft. In the case of steady turning, the deflecting angle of the nozzle of the water jet is

$$\delta(t) = \begin{cases} 0 & 0 < t < t_1 \\ \frac{t-t_1}{t_2-t_1} \delta_0 & t_1 < t < t_2 \\ \delta_0 & t_2 < t \end{cases} \quad (19)$$

## 4.2 Simulation Results

The ALC E40 is taken for numerical simulations. Since the water jet parameters are not available at the time of calculation, these parameters are derived from the literatures. The simulation starts with the craft in a straight course, with the deflecting angle of the nozzle of the water jet gradually increasing to the desired value, and then kept fixed, thus nozzles of the water jets generating a turning moment. Figures 14 to 17 show some of the simulated results of an ALC turning at about 50 knots of speed. From the simulated results, the turning lever can be obtained by (9). The heeling angle is also a part of the output of the simulations. In the HSC Code 2000, it is required that the total heel angle of the craft in the on-cushion mode due to beam wind and due to turning shall be less or equal to  $12^\circ$ . In the present case, the craft heel angle due to turning is about  $1.7^\circ$ , which is far less than the limited value.

Figure 18 shows the heeling angle of the craft in turning at different nozzle deflecting angles. It is found that the heeling angle will increase with increasing deflecting angles. This is not surprising, since larger a nozzle deflecting angle develops larger yaw turning moment and larger turning rate. It is expected that at large deflecting angles, the craft will experience significant heeling and resulting cushion pressure collapse and instability of the craft. Other simulated results (not shown here) indicate that larger nozzle deflecting angle also results higher turning levers that worsen stability. The dependency of turning diameters on craft speed and nozzle deflecting angle of

the water jet are shown in Figures 19 and 20. The turning levers at different speeds are shown in Figure 21. It seems that even through the present model provides reasonable results, it is realised that the above results are based on relatively simple external force models, the hydrodynamic forces are estimates and various parameters are assumed (e.g., water jet). It is expected that further refinement of the model should be made and verified when more accurate forces/parameters are available.

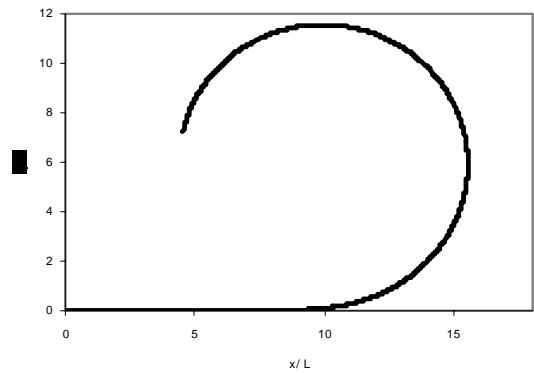


Figure 14 Simulated trajectory of the ALC at 50 knots

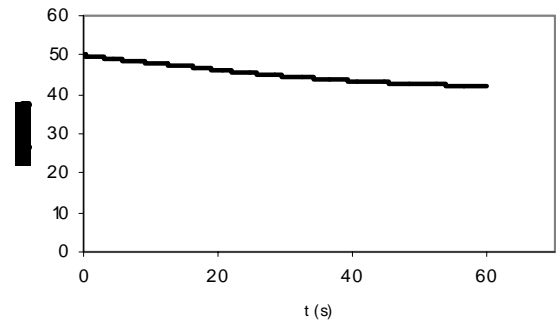


Figure 15 Simulated forward speed

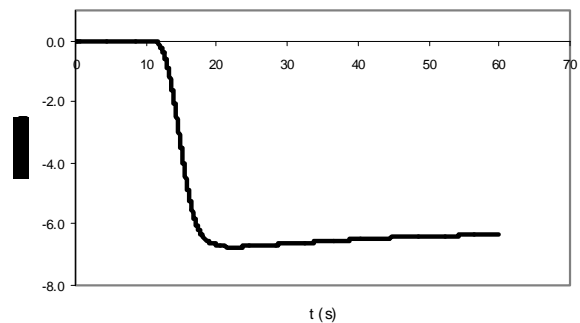


Figure 16 Simulated craft lateral speed

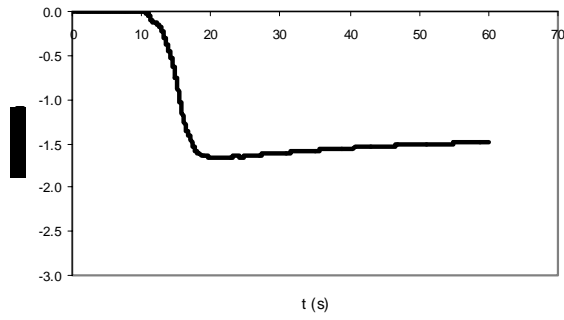


Figure 17 Simulated craft heel angle

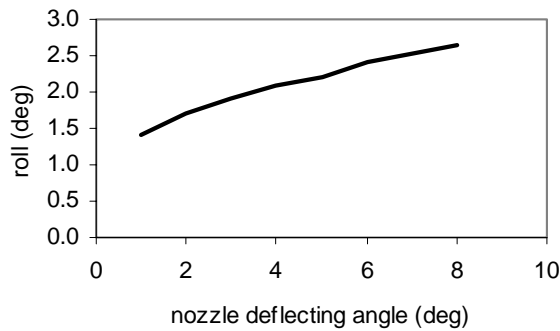


Figure 18 Heel angle of the craft turning at 50knots

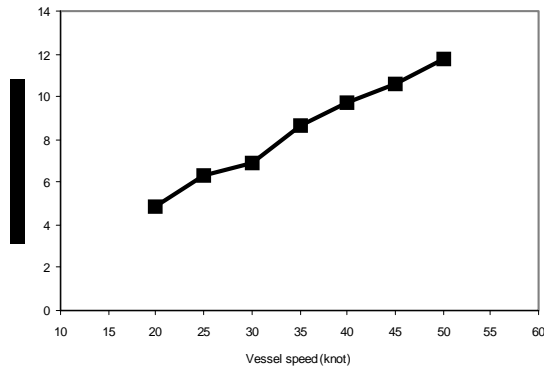


Figure 19 Turning diameter of the ALC at  $\delta_0 = 1.6^\circ$

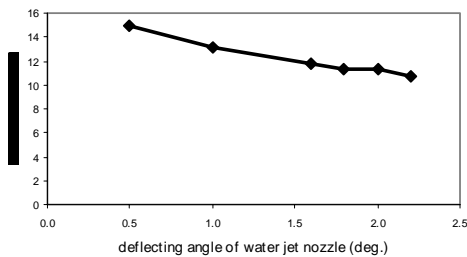


Figure 20 Turning diameter of the ALC at 50knts

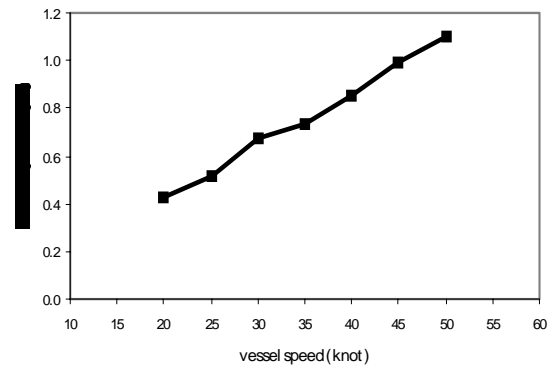


Figure 21 turning level of the ALC at deflecting angle  $\delta_0 = 1.6^\circ$

### 4.3 Directional Stability

The ALC concept is sensible in directional stability due to its design characterises: relatively shallow draught, transom stern, the air chambers and high operational speed. The equations for analysis of directional stability are the same as for turning simulations. An autopilot control law is also incorporated in the form

$$\delta = k_1(\psi - \psi_d) + k_2\dot{\psi} \quad (20)$$

where  $k_1$  and  $k_2$  are the coefficients of the control law, and  $\psi_d$  is the desired vessel direction. Figures 22 ~ 24 show samples of the simulation. In this case, the initial yaw angle of the craft is  $\psi_0 = 10^\circ$  and the desired orientation is  $\psi_d = 0^\circ$ ; initial vessel speed is 50knots. The control parameters are taken to be  $k_1 = 1$  and  $k_2 = 2$ . The simulated results indicate that the vessel can reach its desired orientation in about 20 seconds. Also in this process, the vessel undergoes roll motion due to the moment generated by the water jet. Numerical tests show that the control parameters  $k_1$  and  $k_2$  have a significant effect on the directional stability of the craft. In order to carry out more realistic simulation for the ALC, actual parameters should be used as the input of the simulator.

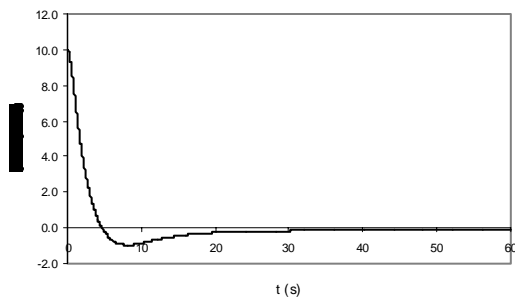


Figure 22 Simulated yaw time history

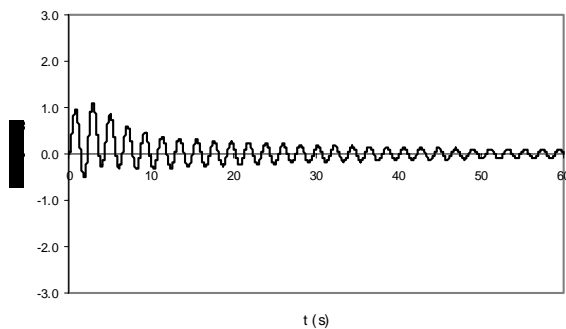


Figure 23 Simulated roll time history

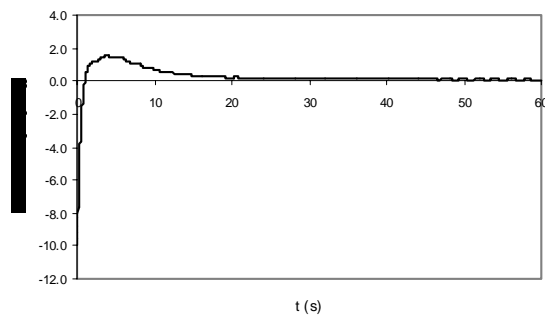


Figure 24 Simulated time history of nozzle deflecting angle

## 5. CONCLUSIONS

This paper presents some stability and safety studies for the Air Lifted Catamaran (ALC) carried out at the Ship Stability Research Centre (SSRC). Numerical prediction tools have been developed for stability analysis of the craft. Some sample results for the E40 concept are presented and discussed. Reasonable results are obtained. The effects of design parameters on the stability are discussed. Those tools could be helpful for the designer and operator of the craft. The stability analysis reported here is mainly for the craft at on-cushion mode. The stability and

survivability of the ALC craft at off-cushion mode (damage case) should be analysed with other methods. It is realized that some of the coefficients in the numerical simulations are empirical, or borrowed from other vessels, this may, in turn, partially affect the accuracy of the present prediction. It is certainly true that the prediction will be improved when more accurate data made available for the ALC.

## 6. ACKNOWLEDGMENTS

The present research was supported by the 5<sup>th</sup> framework EU project EFFISES, the EU funding is gratefully acknowledged.

## 7. REFERENCES

- Aage, C, 1971, "Wind Coefficients for Nine Ship Models", Hydro- or Aerodynamisk Laboratorium, Report No. A-3.
- Allenstrom, B., Liljenberg, H and Tuden, U., 2001, "An Air Lifted Catamaran – Hydrodynamic Aspects", Proceedings of FAST'01, Southampton, U.K. pp.29-40.
- Allenstrom, B., Liljenberg, H and Tuden, U., 2003, "Concept Development and Model Testing – New Generation Air Assisted Vessels (AAV) with Water Jet Propulsion", Proceedings of FAST'03, Italy. Pp.59-68.
- Blyth, A.G., 1993, "The Roll Stability of Surface Effect Ships", Transactions of The Royal Institution of Naval Architects, London, pp271-285.
- Doctors, L.J., 1974, "The Effect of Air Compressibility on the Non-linear Motions of An Air Cushion Vehicle over Waves", Proceedings of 11<sup>th</sup> Symposium on Naval Hydrodynamics, London, pp.373-388.
- Faltinsen, O.M., 2002, "Sea Loads on High Speed Marine Vehicles, NTNU, Trondheim.

---

IMO, 2000, HSC Code 2000, MSC 73/21/ADD.1, adopted Dec. 2000.

Jasionowski, A, 2001, "PROTEUS3 Users Manual", University of Strathclyde, Glasgow.

Kaplan, P., 1995, "Manoeuvring and Stability of SES and Catamaran Ships", Transactions of The Royal Institution Naval Architects. pp.17-36.

Kim, C.H. and Tsakonas, S., 1981, "An Analysis of Heave Added Mass and Damping of a Surface Effect Ship", Journal of Ship Research, Vol. 25, No.1. pp.44-61.

Papanikolaou, A.D., Georgantzi, N and Karayannis, T., 2002, "Adaptation of Stability Rules and Tools to SES", Report of National Technical University of Athens.

Vassalos, D., 1995, "Intact and Damage Stability and Survivability of Advanced Marine Vehicles", University of Strathclyde, Glasgow.

Wade, R. B. and Wang, S., 1977, "Some Aspects of Side-hull Hydrodynamics and Maneuvering in the Design of Surface Effect Ships", Proceedings of 11<sup>th</sup> Symposium on Naval Hydrodynamics, London. pp.355-371.

Xie, N., Vassalos, D. and Jasionowski, A., 2005a, "A Study of Hydrodynamics of Three-dimensional Planing Surface", Ocean Engineering, Vol. 32, pp. 1539-1555.

Xie, N., Vassalos, D. and Jasionowski, A., 2005b, "Seakeeping Analysis of the Air Lifted Vessel", Proceedings of The 4<sup>th</sup> International Workshop on Ship Hydrodynamics, Shanghai, pp. 113-120.

---